ORIGINAL PAPER

Research on the attenuation law of blasting vibration in tunnel engineering

Renliang Shan[1] · Yan Zhao[1] · Hailong Wang[1,2] · Jie Dong[2] · Dongsheng Wang[1]

Abstract

To accurately predict the attenuation law of the blasting vibration velocity, the concept of equivalent radius (rd) is introduced based on Heelan short column charge theory. The attenuation model equation of the peak blasting vibration velocity under the action of the internal instantaneous excitation load is obtained and verified by dimensional analysis. Combined with an example of tunnel blasting engineering, the attenuation law of blasting vibration velocity is studied. In addition, the improved formula under the conditions of spherical charge and cylindrical charge is discussed. The comparison results show that the effect of fitting analysis obtained by the improved formula is the best and can provide a reference for similar blasting projects.

Keywords Blasting vibration velocity · Theoretical analysis · Field experiment · Regression calculation

Introduction

With the rapid development of transportation infrastructure construction, the utilization rate of underground space has significantly increased. The route selection of railway tunnels will inevitably pass through existing buildings. Drilling and blasting are the main methods of mountain tunnel excavation, but the induced blasting vibration adversely affects the surrounding buildings. Therefore, the accurate prediction of rock blasting vibration has important engineering significance to ensure the safety of surrounding buildings (Zheng et al.2021; Alimohammadi et al. 2020; Satvati et al. 2020; Alimohammadi et al. 2019, Zhao et al.2021a).

Most researchers used the peak particle velocity (PPV) as an indicator and conducted research on the response characteristics of blasting vibration. Yu et al. (2021) used similar simulation experiments to study the effect of the

joint weakness on the transmission of blasting vibration. The experimental results showed that the number of joints greatly affected the prediction accuracy of blasting vibration. Roy et al. (2020) studied the influence of the total charge on the intensity of blasting vibration. When the maximum charge is used as a fitting parameter, the prediction effect of blasting vibration is good. Zhao et al. (2021b) obtained a new fitting method for tunnel blasting vibration through induction and dimensional analysis. In addition, the analysis method was used to study the attenuation law of blasting vibration energy. A comparison of four prediction models of blasting vibration velocity shows that the prediction effects of the USBM model and Sadofsky equation are similar and can be widely used in subsequent prfediction work (Ongen et al. 2018). Lu et al. (2018) studied the influence of an airborne free surface on the attenuation law of blasting vibration using actual measurements and numerical analysis. In addition, a large number of on-site monitoring technology and experimental verification methods (Dong et al. 2021, 2017; Sengupta et al. 2021; Gao et al. 2019; Wang et al. 2021) have also been applied in the research for the tunnel engineering. Ji et al. (2021) made statistics on the damage characteristics of tunnel surrounding rock through acoustic wave tests, and proposed corresponding control thresholds. Zhong et al. (2012) used the method of combining dimensional analysis with wavelet packet analysis to study the vibration attenuation law of tunnel and open-air slope collaborative blasting.

Responsible Editor: Longjun Dong

✉ Yan Zhao
  304965624@qq.com

[1] School of Mechanics and Civil Engineering, China University of Mining and Technology (Beijing), Beijing 100083, China

[2] Hebei Provincial Key Laboratory of Civil Engineering Diagnosis, Reconstruction and Disaster Resistance, Hebei University of Architecture, Zhangjiakou 075000, Hebei, China

In summary, most studies predict the attenuation law of blasting vibration through field measurements (Huang et al. 2019; Gou et al. 2020) or numerical simulation (Xu et al. 2019; Yang et al. 2020; Peng et al. 2021). However, there are few theoretical derivation studies on the attenuation law of blasting vibration. The theoretical derivation of blasting vibration is of great significance for comprehensively understanding the transmission of blasting stress waves and accurately predicting the evolution of blasting vibration. Therefore, based on the analytical solution of the wave equation excited by the short column charge, the attenuation model equation of the tunnel blasting vibration is derived. Secondly, the reliability of the improved formula is verified by dimensional analysis. Finally, the two charge expression forms of the two blasting vibration fittings are separately discussed, and the prediction effects of the three fitting methods are compared. The content of this research is dedicated to introducing a new working idea to predict and control blasting vibration in the future and proposes improvements and supplements to traditional prediction methods.

Theoretical analysis of the peak velocity attenuation of blasting vibration

At present, most researchers use the Sadofsky formula (Matidza et al. 2020; Zhao et al. 2021a) or the USBM model (United States Bureau of Mines) (Azimi et al. 2019; Hosseini et al. 2019; Shi et al. 2018; Jayasinghe et al. 2019; Arthur et al. 2020) to fit and analyze the blasting vibration velocity. In addition, other classic models have been used to predict the peak particle velocity.

This empirical formula only considers the influence of the distance from the blast area and the blasting charge on the PPV. It does not reflect the influence of other factors on the PPV, such as charge type, charge radius, drilling radius, blasthole layout, mechanical properties of the medium rock mass, and topographic and geological conditions (Hu et al. 2020; Jiang et al. 2017). Therefore, based on the analytical solution of the wave excited by the short column charge, the attenuation law of blasting vibration in the middle and far fields is studied.

Attenuation law of blasting vibration based on short column charge

When the distance from the blast area is greater than the length of the cylindrical charge and wavelength of the stress wave, Hustrulid et al. (1992) obtained an analytical solution for the low-frequency fluctuations of the short column cavity under instantaneous internal load excitation.

As shown in Fig. 1, assuming that the internal instantaneous excitation load acts on the inner wall of a short
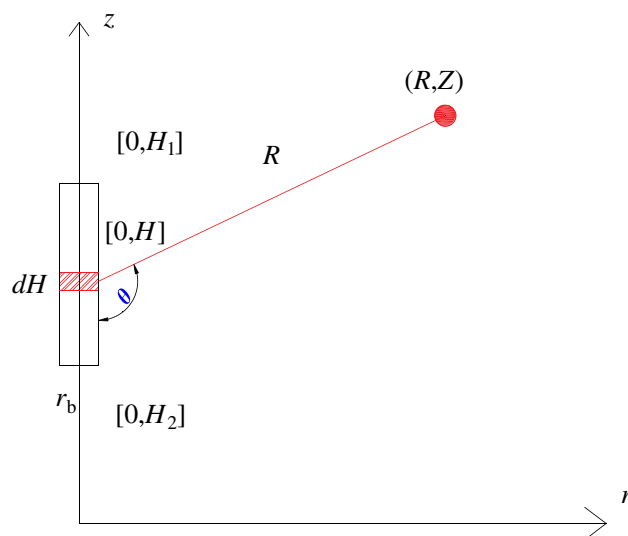

Fig. 1 Instantaneous load acts on the inner wall of the short column cavity with a length of dH

cylindrical cavity with a length of dH and a radius of r_b, the displacement field can be expressed as:

$$u_p = \left(\frac{r_b^2 dH p_0}{4 G c_p R}\right)[1 - (\frac{c_s}{c_p})\cos^2\theta]\left\{\frac{\partial f[t - \frac{(H-H_1)}{D} - \frac{R}{c_p}]}{\partial t}\right\} \quad (1)$$

$$u_s = \left(\frac{r_b^2 dH p_0 \sin\theta\cos\theta}{2 G c_s R}\right)\left\{\frac{\partial f[t - \frac{(H-H_1)}{D} - \frac{R}{c_s}]}{\partial t}\right\} \quad (2)$$

where u_p is the displacement caused by the compression wave; u_s is the displacement caused by the shear wave; r_b is the radius of the charge; p_0 is the initial pressure of the blasthole; G is the shear modulus of the rock; D is the propagation speed of the detonation wave; R is the distance between the vibration source and the measuring point; t is the time of action; H_1 and H_2 are the upper and lower limits of the calculation of H; c_p and c_s are the propagation velocities of the compression wave and shear wave, respectively.

Then, the radial displacement and vertical displacement excited by the explosion of the short column charge can be expressed as

$$u_r = u_p\sin\theta + u_s\cos\theta \quad (3)$$

$$u_z = -u_p\cos\theta + u_s\sin\theta \quad (4)$$

where u_r and u_z are the radial vertical displacement excited by the instantaneous load.

The velocity field excited by the instantaneous load can be obtained by differential calculation:

$$\begin{cases} V_r = \frac{\partial u_r}{\partial t} \\ V_z = \frac{\partial u_z}{\partial t} \end{cases} \tag{5}$$

Many scientific studies (Jiang et al. 2012; Ji et al. 2021; Luo et al. 2021) have shown that the S wave is the dominant wave near blasting, which mainly controls the surrounding rock damage caused by blasting construction. The P wave is an important part of the blasting near zone and blasting far zone, and it mainly affects the blasting vibration in the middle and far zones of blasting. However, it is well known that P waves decay faster than S waves. Therefore, the S wave may dominate the vibration in the far region. Based on the above analysis, the common contribution of P wave and S wave to vibration should be considered.

$$\begin{cases} V_p = \frac{k_1 dH p_0}{\rho c_p R} \\ V_s = \frac{k_2 dH p_0}{\rho c_s R} \end{cases} \tag{6}$$

where ρ is the rock density, and $k1$ and $k2$ are undetermined coefficients. The PPV caused by the short column charge is:

$$V = \int_H \overline{V}_p ds + \int_H \overline{V}_s ds \tag{7}$$

In particular, the result of formula (7) refers to the vector sum of the two velocities.

Simplifying formula (7), we obtain:

$$V = k(\frac{r_b}{R})(\frac{p_0}{\rho c_p}) \tag{8}$$

Since the actual rock mass has viscoelastic and damping properties, the blasting vibration attenuation equation of the actual rock mass can be expressed as:

$$V = k(\frac{r_b}{R})^\alpha (\frac{p_0}{\rho c_p}) \tag{9}$$

The vibration speed on the blasthole wall can be expressed as:

$$V_0 = \frac{p_0}{\rho c_p} \tag{10}$$

Equation (10) can also be expressed as:

$$V = k(\frac{r_b}{R})^\lambda V_0 \tag{11}$$

where k is the site coefficient, λ is the attenuation coefficient, rb is the radius of the cylindrical charge, and R is the distance from the blast area.

Improvement of blasting vibration velocity fitting formula

Equation (11) is indicated to be suitable for single-hole blasting, but it is relatively difficult to obtain engineering parameters in the formula. In addition, multi-hole and multi-stage blasting is often used in tunnel blasting engineering, and single-hole blasting is rare. Therefore, an attempt is made to find an equivalent solution suitable for tunnel blasting.

Determination of equivalent boundary of blasting

According to the difference in stress state, the rock mass near the blasting source can be divided into a crushed zone, fractured zone, and elastic zone. The actual blasting vibration test is often located in the elastic zone. The rock mass in this area can be approximated as an elastic body, while the rock mass in the crushed zone and the fractured zone is seriously damaged by the blast stress wave. However, the boundary of the inelastic zone can be considered the blasting load equivalent boundary (Deng et al. 2020; Irazoqui et al. 2000) to study the propagation law of blasting vibration.

Under the condition of a single blasthole cylindrical charge, the radius of the crushed zone ($r1$) and radius of the fractured zone ($r2$) can be expressed as (Yang et al. 2012):

$$r_1 = \left(\frac{p c_p{}^2}{5\sigma_c}\right)^{\frac{1}{2}} \left(\frac{p_0}{\sigma^*}\right)^{\frac{1}{4}} r_b \tag{12}$$

$$r_2 = \left(\frac{\mu p_0}{(1-\mu)\sigma_t}\right)^{\frac{1}{\beta}} r_b \tag{13}$$

where σc and σt are the dynamic uniaxial compressive strength and dynamic uniaxial tensile strength of the rock mass, respectively; σ^* is the dynamic compressive strength of the rock mass under multi-directional stress conditions; β is the propagation attenuation coefficient; μ is Poisson's ratio of the rock. Generally, the radius of the crushed zone is 3~5 times the radius of the charge, and the radius of the fractured zone is 10~15 times the radius of the charge.

If the interaction between the blastholes is not considered, the detonation of each cutting hole can be approximated as a short cylindrical cavity subjected to internal transient loads in a semi-infinite medium. Therefore, the effective boundary of the cutting section initiation can be approximated as the envelope of the multi-hole blasting fractured zone (Esen et al. 2003; Liang et al. 2013).
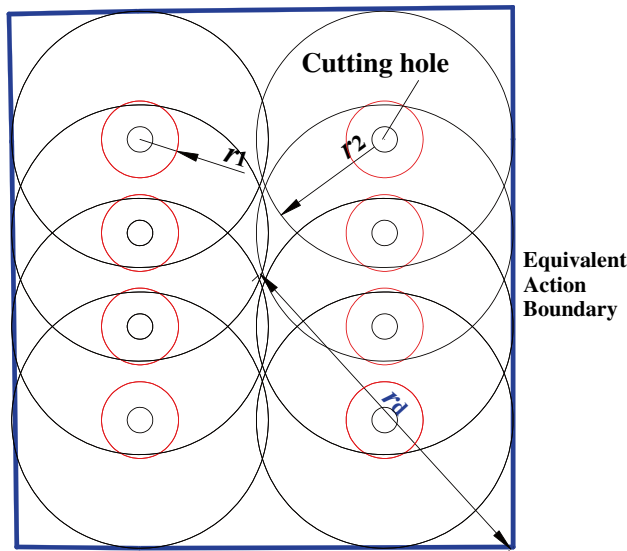
Fig. 2 Schematic diagram of the equivalent boundary of cutting hole blasting

Non-cutting holes, such as auxiliary holes, penetrate through the axis of adjacent blastholes to destroy the thrown rock, and their void surface can be approximated as an equivalent boundary. Figure 2 is a schematic diagram of the equivalent radius (rd) of the cutting hole of the tunnel blasting.

Determination of the equivalent load of blasting load

According to the theory of detonation waves C-J of condensed charge, the initial detonation pressure $p0$ on the blasthole wall can be expressed as:

$$p_0 = \frac{\rho_e D^2}{2(\gamma + 1)} \tag{14}$$

Under the condition of uncoupling charge, the initial detonation pressure on the blasthole wall is:

$$p_0 = \frac{\rho_e D^2}{2(\gamma + 1)} \left(\frac{d_a}{d_b} \right)^{2\gamma} \tag{15}$$

If the uncoupling coefficient is large, the explosion gas expansion must go through two processes.

$$\begin{cases} \gamma = 3 & p_0 \geq p_e \\ \gamma = \upsilon = \frac{4}{3} & p_0 < p_e \end{cases} \tag{16}$$

where pe is the critical pressure of the explosive gas.

The initial detonation pressure can be expressed as follows:

$$p_0 = \left(\frac{\rho_e D^2}{2(\gamma + 1)} \right)^{\frac{\upsilon}{\gamma}} \left(\frac{d_a}{d_b} \right)^{2\gamma} p_e^{\frac{(\gamma - \upsilon)}{\gamma}} \tag{17}$$

where ρe is the explosive density, γ is the isentropic coefficient of the explosive, and da and db are the diameters of the cylindrical charge and the blasthole, respectively.

The variation law of the blasting load of a single blasthole with the distance from the blast area is:

$$p_d = p_0 \left(\frac{R}{r_b} \right)^{-\xi} \tag{18}$$

where ζ is the load transmission index; for the crushed zone, $\zeta = 2 + \mu/1 - \mu$; for the fractured zone, $\zeta = 2 - \mu/1 - \mu$.

Considering the influence of the group of holes in the cutting section on the equivalent blasting load, η is introduced as the influence coefficient of the blast load to simultaneously initiate multiple holes:

$$\eta = n \left(\frac{r_2}{r_d} \right)^2 \tag{19}$$

where n is the number of blastholes in the cutting section.

For the cutting section with multiple simultaneously detonated blastholes, the equivalent blasting load is:

$$p_d = \eta p_0 \left(\frac{r_1}{r_b} \right)^{-2 - \frac{\mu}{1-\mu}} \left(\frac{r_2}{r_1} \right)^{-2 + \frac{\mu}{1+\mu}} \tag{20}$$

For noncutting holes, the blasting load is equivalently applied to the plane where the centerline of the blasthole and the axis of the blasthole are located. The equivalent load size is:

$$p_d = \frac{2r_b p_0}{s} \tag{21}$$

where s is the distance between adjacent blastholes.

Then, the improved attenuation equation for the vibration velocity can be written as:

$$\begin{cases} V_0 = \frac{p_d}{\rho c_p} \\ V = k \left(\frac{r_d}{R} \right)^\lambda V_0 \end{cases} \tag{22}$$

Dimensional analysis

To verify the feasibility of the improved formula (22), a dimensional analysis is used to derive the velocity attenuation equation of tunnel blasting vibration. Among the influencing factors, the rock density (ρ), longitudinal wave propagation velocity (cp), distance from the blast area (R), rock elastic modulus (E), and blasting load equivalent radius

(*rd*) are selected as the main influencing factors. Moreover, cp, R, and ρ are selected as independent dimensions; then:

$$V = \varphi\left(\rho, c_p, R, r_d, E\right) \tag{23}$$

According to the π theorem, Eq. (23) can be represented by 3 dimensionless numbers:

$$\begin{cases} \pi_1 = \frac{V}{c_p} \\ \pi_2 = \frac{r_d}{R} \\ \pi_3 = \frac{E}{c_p^2 \rho} \end{cases} \tag{24}$$

Therefore:

$$\frac{V}{c_p} = \Pi\left\{\frac{E}{c_p^2 \rho}, \left(\frac{r_d}{R}\right)\right\} \tag{25}$$

According to the dimensional harmony theorem:

$$\frac{V}{c_p} = K\left(\frac{E}{c_p^2 \rho}\right)^\alpha \left(\frac{r_d}{R}\right)^\beta \tag{26}$$

For a specific tunnel project, E, cp, and ρ remain basically unchanged, so they can be converted into:

$$V = K\left(\frac{r_d}{R}\right)^\omega \tag{27}$$

Equation (27) has the same form as the improved formula (22), which verifies the feasibility of the improved formula.

Project background and monitoring plan

The blasting project of Chong-li Tunnel was used as the engineering background for subsequent research. The main tunnel passes through the existing villages with a minimum vertical clearance of 18 m. The surrounding rock of the tunnel is designed to be grade III. Figure 3 shows the topographic map of the underpass section of the Chong-li Tunnel.

Blasting construction plan

According to the surrounding rock grade and geological conditions of the tunnel, the tunnel is driven by full-face blasting, as shown in Fig. 4. Table 1 shows the specific charge of blasting construction. The density of the surrounding rock is 2630 kg/m3, the longitudinal wave velocity is approximately 5500 m/s, the detonation wave velocity is 4500 cm/s, and the explosive density is 1 g/cm3.

Blasting vibration monitoring program

A TC-4850 N blasting vibration tester was used in the on-site monitoring process. The blasting vibration meter is equipped with the three-axis vibration velocity sensor TCS-B3, which can simultaneously collect the blasting vibration velocity in the three directions of *X*, *Y*, and *Z*. As shown in Fig. 5, the five measurement points horizontally adjacent to the tunnel were selected for this monitoring.

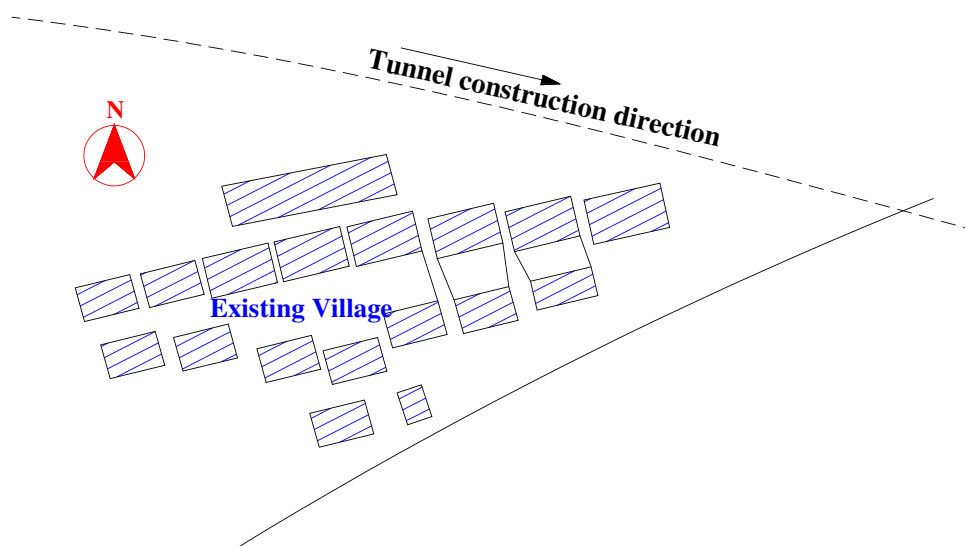**Fig. 3** Topographic map of the underpass section of the tunnel
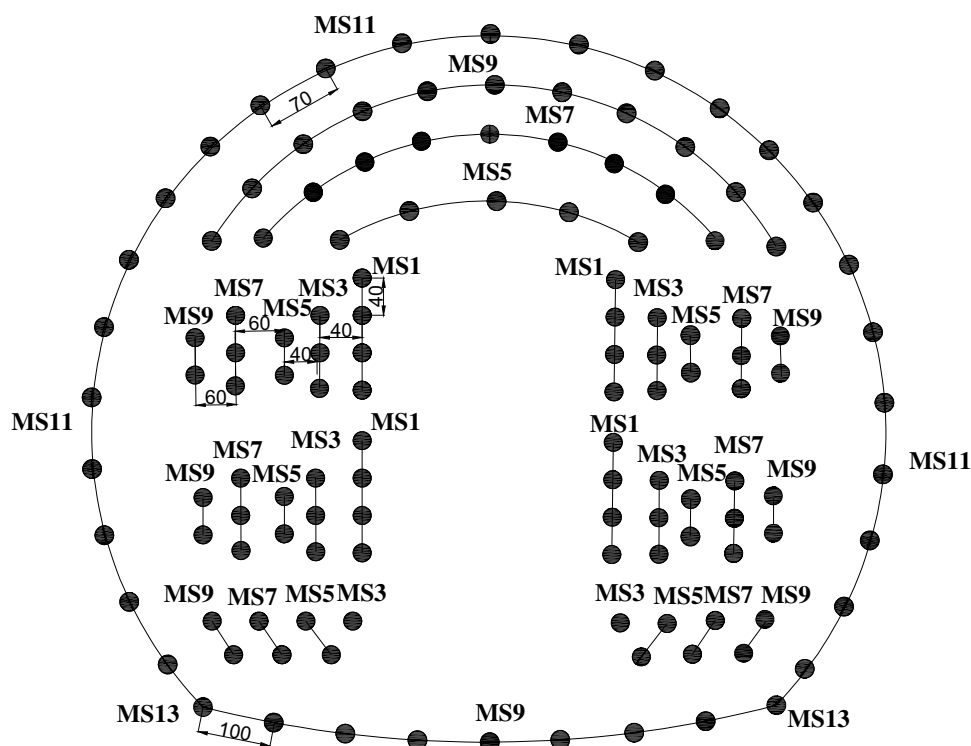
Fig. 4 Layout of the blasthole

Table 1 Specific charge for tunnel blasting

Type of blasthole	Blasthole depth (m)	Detonator level (segment)	Number of holes (number)	Single-hole charge (kg)	Total charge (kg)
Cutting hole	4.0	MS1	16	2.7	43.2
Auxiliary hole	3.5	MS3	8	2.4	19.2
Auxiliary hole	3.5	MS5	17	1.8	30.6
Auxiliary hole	3.5	MS7	25	1.5	37.5
Auxiliary hole	3.5	MS9	30	1.5	45
Peripheral hole	2.5	MS11	25	1.2	30
Bottom plate hole	2.5	MS13	2	2.1	4.2
			123		209.7

Regression analysis of on-site measurement results

Table 2 is the results of two field experiments. As shown in Fig. 6, the blasting vibration speed excited by each detonator can be clearly distinguished from the waveform time history diagram.

Table 2 shows that the vibration velocity in the *Z* direction is the largest among the three directions. Therefore, the subsequent analysis only focuses on the velocity in the *Z* direction. In addition, the PPVs corresponding to MS1 and MS9 are the largest. The PPVs corresponding to MS1 of the two blasting constructions are 1.99 cm/s and 2.33 cm/s, respectively. For comparison, the PPVs corresponding to MS9 are 1.58 cm/s and 2.02 cm/s,

respectively. To predict the blasting vibration accurately, classification research should be conducted according to the blasthole type.

Regression analysis of PPV

Equation (22) is used in the regression calculation of the blasting vibration velocity, and the fitting results are shown in Fig. 7. It shows that Eq. (22) has a good fitting effect on the PPV induced by different detonator positions, and all correlation coefficients are greater than 0.8.

Figure 7 shows that the same model equation can express the PPV that corresponds to the same type of blastholes. For example, the PPV excited by multiple-level detonators in the auxiliary hole shows a good linear fitting relationship, and the correlation coefficient is as

Fig. 5 Layout of measuring points
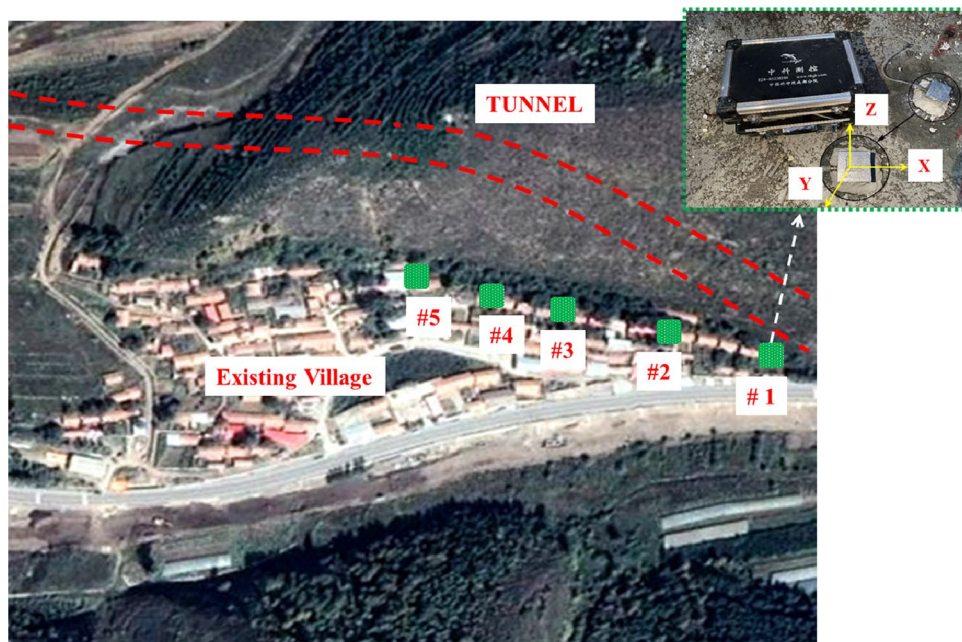
Table 2 Peak blasting vibration velocity (PPV) and related parameters

Measuring point	Experiment	R (m)	PPV (cm/s)						
			Cutting hole	Auxiliary hole				Peripheral hole	Bottom plate hole
			MS1	MS3	MS5	MS7	MS9	MS11	MS13
5#	I	27.58	1.99	1.04	1.22	1.29	1.58	0.84	0.38
4#		30.48	1.66	0.87	0.91	1.08	1.27	0.73	0.25
3#		36.89	1.34	0.72	0.46	0.89	1.23	0.62	0.20
2#		40.31	1.11	0.64	0.58	0.80	0.92	0.57	0.22
1#		49.24	0.98	0.56	0.48	0.61	0.76	0.46	0.23
5#	II	20.39	2.33	1.2	1.61	1.68	1.95	1.25	0.70
4#		21.54	2.22	1.03	1.24	1.65	1.67	0.99	0.48
3#		25.26	2.01	0.97	1.15	1.50	2.02	1.14	0.44
2#		28.28	1.96	0.88	0.91	1.16	1.35	0.85	0.34
1#		36.48	1.55	0.89	0.80	1.12	1.28	0.69	0.26

high as 0.8770. Thus, it is feasible to uniformly fit and analyze the vibration velocities induced by the same type of blastholes, which saves calculation time and obtains a blasting vibration attenuation law that is more consistent with reality.

Form of charge of attenuation formula

To verify the superiority of the introduced fitting Eq. (22), a comparative analysis was conducted by introducing a common charge structure. For spherical charge blasting at one time, the charge quantity has the following relationship with the equivalent radius (Liu et al. 2018).

$$Q = \frac{4}{3}\pi q \mathrm{r}_d{}^3 \tag{28}$$

Therefore, Eq. (22) can be rewritten as:

$$\begin{cases} V_0 = \frac{p_d}{\rho c_p} \\ V = k\left(\frac{\sqrt[3]{Q}}{R}\right)^\lambda V_0 \end{cases} \tag{29}$$

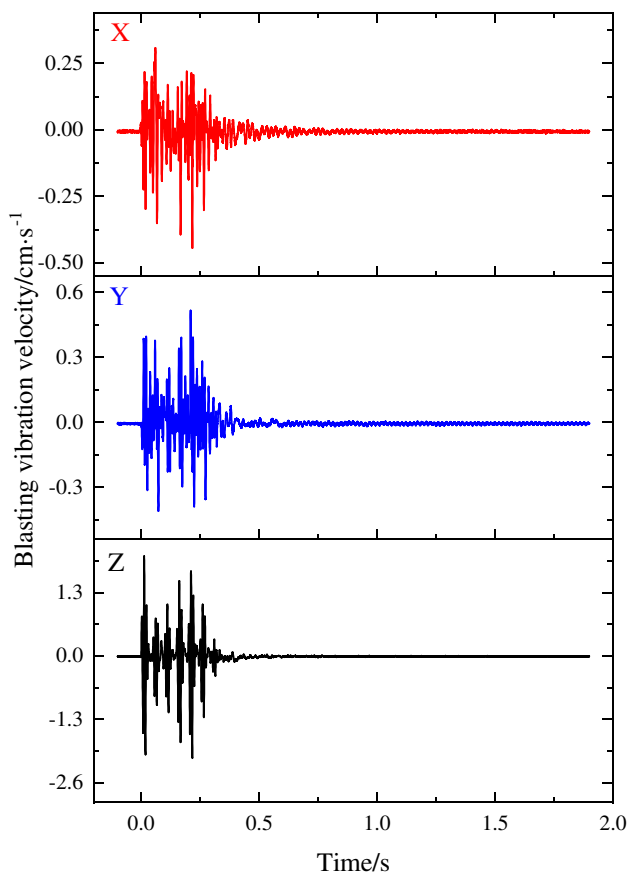Similarly, for the columnar charge, Eq. (22) can be rewritten as:

Fig. 6 Time-history waveform of the blasting vibration of the experiment

$$\begin{cases} V_0 = \frac{p_d}{\rho c_p} \\ V = k\left(\frac{\sqrt{Q}}{R}\right)^\lambda V_0 \end{cases} \tag{30}$$

The regression analysis of the test data is performed using Eqs. (29) and (30). The comparison with the fitting effect of Eq. (22) is summarized in Table 3.

Table 3 shows that all correlation coefficients of Eqs. (29)~(30) are smaller than those of Eq. (22), but the correlation coefficients of cutting holes, peripheral holes, and bottom plate holes are not significantly different. However, for the auxiliary hole, the fitting coefficients obtained by Eqs. (29)~(30) are 0.4976 and 0.4370, respectively, which are much smaller than those obtained by Eq. (22). The above analysis proves that the charge form of the attenuation equation is better in fitting the blasting vibration induced by single-segment detonators, but it is not suitable for analyzing blasting vibrations corresponding to multi-segment detonators. The main reason for this difference is that the initiation of cutting holes, etc. is mainly affected by the maximum charge per delay. However, the auxiliary hole is composed of multiple sections of detonators, which makes the vibration speed that is excited by different levels have obvious differences. If the maximum charge per delay is used as the fitting parameter, it cannot truly reflect the law of blasting vibration.

Fig. 7 Fitting of attenuation of blasting vibration particles
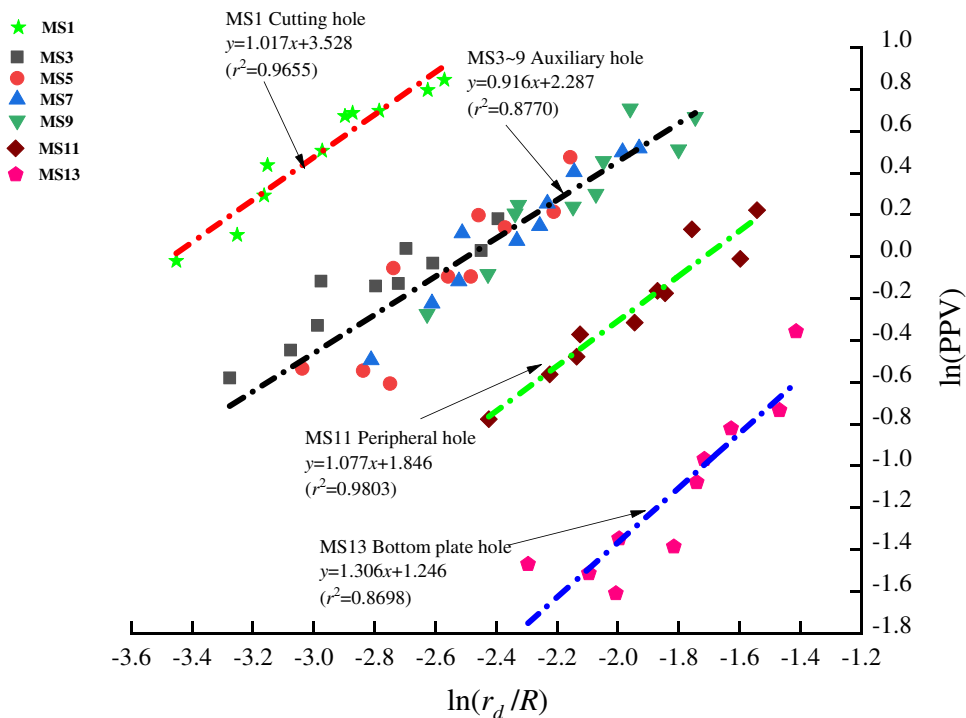
Table 3 Fitting formula of blasting vibration

Fitting model	Type of blasthole	Fitting equation	Correlation coefficient
Equation (22)	Cutting hole	$PPV = 34.06\left(\frac{r_d}{R}\right)^{1.02}$	0.9655
	Auxiliary hole	$PPV = 9.85\left(\frac{r_d}{R}\right)^{0.916}$	0.8770
	Peripheral hole	$PPV = 6.35\left(\frac{r_d}{R}\right)^{1.08}$	0.9803
	Bottom plate hole	$PPV = 3.48\left(\frac{r_d}{R}\right)^{1.31}$	0.8698
Equation (29)	Cutting hole	$PPV = 14.92\left(\frac{\sqrt[3]{Q}}{R}\right)^{1.017}$	0.9255
	Auxiliary hole	$PPV = 4.10\left(\frac{\sqrt[3]{Q}}{R}\right)^{0.5812}$	0.4976
	Peripheral hole	$PPV = 9.12\left(\frac{\sqrt[3]{Q}}{R}\right)^{1.08}$	0.9204
	Bottom plate hole	$PPV = 16.11\left(\frac{\sqrt[3]{Q}}{R}\right)^{1.31}$	0.7827
Equation (30)	Cutting hole	$PPV = 7.89\left(\frac{\sqrt{Q}}{R}\right)^{1.02}$	0.9255
	Auxiliary hole	$PPV = 4.26\left(\frac{\sqrt{Q}}{R}\right)^{0.86}$	0.4370
	Peripheral hole	$PPV = 4.95\left(\frac{\sqrt{Q}}{R}\right)^{1.08}$	0.9203
	Bottom plate hole	$PPV = 12.18\left(\frac{\sqrt{Q}}{R}\right)^{1.30}$	0.7927

Conclusion

Based on the analytical solution of the stress wave of the short column charge, the blasting vibration attenuation formula is deduced. Relying on specific blasting projects, a regression analysis was performed, and the following conclusions were obtained:

1. Based on short column charge theory, the concept of equivalent radius is introduced, and the blasting vibration attenuation model equation is theoretically deduced. It is verified through dimensional analysis.
2. The improved model can accurately predict the peak blasting vibration velocity for different detonator positions and apply to the fitting analysis of the PPV for different blasthole types.
3. By comparison, the fitting effect of the two charge forms of the blasting vibration attenuation formula is not as good as the improved formula, which proves that the attenuation model of blasting vibration introduced is suitable for practical engineering.

Declarations

Conflict of interest The authors declare no competing interests.

References

Alimohammadi H, Dastjerdi KY, Yaghin ML (2020) The study of progressive collapse in dual systems. Civ Environ Eng 16:79–85. https://doi.org/10.2478/cee-2020-0009

Alimohammadi H, Esfahani MD, Yaghin ML (2019) Effects of openings on the seismic behavior and performance level of concrete shear walls. International Journal of Engineering and Applied Sciences (IJEAS) 6 https://doi.org/10.31873/IJEAS.6.10.10

Arthur CK, Temeng VA, Ziggah YY (2020) Multivariate adaptive regression splines (MARS) approach to blast-induced ground vibration prediction. Int J Min Reclam Environ 34:198–222. https://doi.org/10.1080/17480930.2019.1577940

Azimi Y, Khoshrou SH, Osanloo M (2019) Prediction of blast induced ground vibration (BIGV) of quarry mining using hybrid genetic algorithm optimized artificial neural network. Measurement 147:106874. https://doi.org/10.1016/j.measurement.2019.106874

Chi LY, Zhang Z, Aalberg A, Li CC (2019) Experimental investigation of blast-induced fractures in rock cylinders. Rock Mech Rock Eng 52:2569–2584. https://doi.org/10.1007/s00603-019-01749-0

Deng X, Wang J, Wang R, Liu Q (2020) Influence of blasting vibrations generated by tunnel construction on an existing road. Int J Civ Eng 18:1381–1393. https://doi.org/10.1007/s40999-020-00549-w

Dong LJ, Shu WW, Sun DY, Li XB, Zhang LY (2017) Pre-alarm system based on real-time monitoring and numerical simulation using Internet of Things and cloud computing for tailings dam in mines. IEEE ACCESS 5:21080–21089. https://doi.org/10.1109/ACCESS.2017.2753379

Dong L, Tong X, Hu Q, Tao Q (2021) Empty region identification method and experimental verification for the two-dimensional complex structure. Int J Rock Mech Min 147:104885. https://doi.org/10.1016/j.ijrmms.2021.104885

Esen S, Onederra I, Bilgin HA (2003) Modelling the size of the crushed zone around a blasthole. Int J Rock Mech Min 40:485–495. https://doi.org/10.1016/S1365-1609(03)00018-2

Gao Q, Lu W, Yang Z, Chen M, Yan P (2019) Components and evolution laws of seismic waves induced by vertical-hole blasting. Chin J Rock Mech Eng 38(01):15–27

Gou Y, Shi X, Zhou J, Qiu X, Chen X, Huo X (2020) Attenuation assessment of blast-induced vibrations derived from an underground mine. Int J Rock Mech Min 127:104220. https://doi.org/10.1016/j.ijrmms.2020.104220

Hosseini SA, Tavana A, Abdolahi SM, Darvishmaslak S (2019) Prediction of blast-induced ground vibrations in quarry sites: a comparison of GP, RSM and MARS. Soil Dyn Earthq Eng 119:118–129. https://doi.org/10.1016/j.soildyn.2019.01.011

Hu Y, Yang Z, Huang S, Lu W, Zhao G (2020) A new safety control method of blasting excavation in high rock slope with joints. Rock Mech Rock Eng 53:3015–3029. https://doi.org/10.1007/s00603-020-02113-3

Huang D, Cui S, Li X (2019) Wavelet packet analysis of blasting vibration signal of mountain tunnel. Soil Dyn Earthq Eng 117:72–80. https://doi.org/10.1016/j.soildyn.2018.11.025

Hustrulid W, Bennett R, Ashland F, Lenjani M (1992) A new method for predicting the extent of the blast damaged zone [A]. Proceeding of the Sprangteknisk Konferens [C] , Nitro Nobel, Goteberg-Kiel, Jan 15–16, 55.

Irazoqui HA, Isla MA, Cassano AE (2000) Simplified extense source model for photoreactor analysis and design. Ind Eng Chem Res 39:4260–4271. https://doi.org/10.1021/ie9907876

Jayasinghe B, Zhao Z, Teck Chee AG, Zhou H, Gui Y (2019) Attenuation of rock blasting induced ground vibration in rock-soil interface. J Rock Mech Geotech Eng 11:770–778. https://doi.org/10.1016/j.jrmge.2018.12.009

Ji L, Zhou C, Lu S, Jiang N, Gutierrez M (2021) Numerical studies on the cumulative damage effects and safety criterion of a large cross-section tunnel induced by single and multiple full-scale blasting. Rock Mech Rock Eng. https://doi.org/10.1007/s00603-021-02630-9

Jiang NN, Zhou C, Luo G, Miao G (2012) Blasting vibration safety criterion of railway tunnel concrete lining. J Central South Univ (Sci Technol) 43(07):2746–2750

Jiang N, Zhou C, Lu S, Zhang Z (2017) Propagation and prediction of blasting vibration on slope in an open pit during underground mining. Tunn Undergr Sp Tech 70:409–421. https://doi.org/10.1016/j.tust.2017.09.005

Liang Q, Li J, Li D, Ou E (2013) Effect of blast-induced vibration from new railway tunnel on existing adjacent railway tunnel in Xinjiang. China Rock Mech Rock Eng 46:19–39. https://doi.org/10.1007/s00603-012-0259-5

Liu D, Lu WB, Chen M (2018) Attenuation formula of the dominant frequency of blasting vibration during tunnel excavation. Chin J Rock Mech Eng 37(09):2015–2026. https://doi.org/10.13722/j.cnki.jrme.2018.0311

Lu W, Leng Z, Hu H, Chen M, Wang G (2018) Experimental and numerical investigation of the effect of blast-generated free surfaces on blasting vibration. Eur J Environ Civ En 22:1374–1398. https://doi.org/10.1080/19648189.2016.1262285

Luo S, Yan P, Lu W, Chen M, Wang G, Lu A, Liu X (2021) Effects of in-situ stress on blasting damage during deep tunnel excavation. Arab J Sci Eng 46:11447–11458. https://doi.org/10.1007/s13369-021-05569-9

Matidza MI, Jianhua Z, Gang H, Mwangi AD (2020) Assessment of blast-induced ground vibration at Jinduicheng Molybdenum Open Pit Mine. Nat Resour Res 29:831–841. https://doi.org/10.1007/s11053-020-09623-5

Ongen T, Karakus D, Konak G, Onur AH (2018) Assessment of blast-induced vibration using various estimation models. J Afr Earth Sci 145:267–273. https://doi.org/10.1016/j.jafrearsci.2018.05.004

Peng Y, Liu G, Wu L, Zuo Q, Liu Y, Zhang C 2021 Comparative study on tunnel blast-induced vibration for the underground cavern group. Environ. Earth Sci. 80 https://doi.org/10.1007/s12665-020-09362-z

Roy MP, Mishra AK, Agrawal H, Singh PK 2020 Blast vibration dependence on total explosives weight in open-pit blasting. Arab. J. Geosci. 13 https://doi.org/10.1007/s12517-020-05560-y

Satvati S, Alimohammadi H, Rowshanzamir M, Hejazi SM (2020) Bearing capacity of shallow footings reinforced with braid and geogrid adjacent to soil slope. Int J Geosynth Ground Eng 6:41. https://doi.org/10.1007/s40891-020-00226-x

Sengupta A, Banerjee R, Bandyopadhyay S, 2021 Estimation of ground vibration and settlement during underground tunneling in Kolkata, India. Arab. J. Geosci. 14 https://doi.org/10.1007/s12517-020-06246-1

Shi ZM, Liu L, Peng M, Liu CC, Tao FJ, Liu CS (2018) Non-destructive testing of full-length bonded rock bolts based on HHT signal analysis. J Appl Geophys 151:47–65. https://doi.org/10.1016/j.jappgeo.2018.02.001

Wang, H., Bai, H., Zhao, Y., Wang, D., Wang, X., Wang, S., 2021. The removal method of the blasting vibration signal trend item and noise. Shock Vib. 1-10. https://doi.org/10.1155/2021/1645380.

Xu J, Kang Y, Wang X, Feng G, Wang Z (2019) Dynamic characteristics and safety criterion of deep rock mine opening under blast loading. Int J Rock Mech Min 119:156–167. https://doi.org/10.1016/j.ijrmms.2019.04.015

Yang JH, Lu WB, Chen M, Zhou CB (2012) An equivalent simulation method for blasting vibration of surrounding rock. Explosion and Shock 32(02):157–163. https://doi.org/10.3969/j.issn.1001-1455.2012.02.007

Yang J, Dai J, Yao C, Jiang S, Zhou C, Jiang Q (2020) Estimation of rock mass properties in excavation damage zones of rock slopes based on the Hoek-Brown criterion and acoustic testing. Int J Rock Mech Min 126:104192. https://doi.org/10.1016/j.ijrmms.2019.104192

Yu C, Yue H, Li H, Xia X, Liu B (2021) Scale model test study of influence of joints on blasting vibration attenuation. B Eng Geol Environ 80:533–550. https://doi.org/10.1007/s10064-020-01944-2

Zhao Y, Shan R, Wang H, Tong X, Li Y 2021a. Regression analysis of the blasting vibration effect in cross tunnels. Arab. J. Geosci. 14 https://doi.org/10.1007/s12517-021-08257-y

Zhao Y, Shan RL, Wang HL 2021b Research on vibration effect of tunnel blasting based on an improved Hilbert-Huang transform. Environ. Earth Sci. 80 https://doi.org/10.1007/s12665-021-09506-9

Zheng J, He H, Alimohammadi H (2021) Three-dimensional Wadell roundness for particle angularity characterization of granular soils. Acta Geotech 16:133–149. https://doi.org/10.1007/s11440-020-01004-9

Zhong G, Ao L, Zhao K (2012) Influence of explosion parameters on wavelet packet frequency band energy distribution of blast vibration. J Central South Univ 19(9):2674–2680